Integrated modeling and control of a load-connected SOFC-GT autonomous power system

Rambabu Kandepu, Bjarne A. Foss and Lars Imsland

Abstract— **In this paper we have developed low complexity, control-relevant models of all the components of the SOFC-GT hybrid system which is connected to a load through a bus bar. A control structure is designed by analyzing the complete system and simulation results are presented.**

I. INTRODUCTION

In the foreseeable future, fossil fuels including natural gas will be a major source of energy. With today's increasing concern about global warming and climate change, there is an incentive to investigate natural gas power processes that operate efficiently, thus emitting less per kWh produced, and also power production processes with CO_2 capture capabilities. It is widely accepted that fuel cells are power sources that will become increasingly important, due to high efficiency, low levels of pollution and noise, and high reliability. One of the most promising fuel cell technologies is the Solid Oxide Fuel Cell (SOFC), due to its solid state design and internal reforming of gaseous fuels, in addition to its high efficiency [8]. The SOFC converts the chemical energy of a fuel directly to electrical energy. Since SOFCs operate at high temperatures (about 1000°C), natural gas can be used directly as fuel. The electrical efficiency of a SOFC can reach 55%. Another significant advantage of the SOFC is that since it operates at high temperature and its efficiency increases when pressurized, it naturally lends itself as a heat source for a gas turbine (GT) cycle. The combined (hybrid) cycle can theoretically have an overall electrical efficiency of up to 70%. with a power range from a few hundred kWs to a few MWs [8]. Processes based on SOFCs can be used as power processes with CO_2 capture, since the "used fuel" (and water) and air exit streams can be kept separated [6]. The main applications of the hybrid system include remote area power supply and distributed power generation.

There are several models available in literature for the SOFC-GT hybrid system [11], [2], [9], [19]. In [4], a dynamic model of grid connected SOFC model is developed. However, to the best of authors' knowledge there is no model in the literature with integration of a SOFC-GT hybrid system with a power grid and an electrical load. The reason for procuring an integrated model is to obtain a comprehensive understanding of the operability of the system which has close dynamic interactions between the power generation system and the local grid. Further, the hybrid system consists of tightly integrated dynamic subsystems with strict operating criteria making the control design more challenging in terms of disturbance rejection, part-load operation and in particular start-up, shutdown and load shedding. Suitable system actuation must be chosen, good control structures must be devised, and good controllers must be designed. As a basis for all these tasks, control relevant models must be developed for the subsystems, and for the total system. Such models should have limited complexity to allow for the necessary analysis, and at the same time should include the important dynamic interactions.

In this paper we present an integrated model of a SOFC-GT hybrid system with a power grid connecting to an electrical load. The process is described on a system level and modeling of each component is discussed including the main underlying assumptions. The model is subsequently used to perform analysis of system dynamics and optimize system design. A simple control design is proposed and assessed through a set of simulation scenarios.

II. PROCESS DESCRIPTION

A schematic diagram of the integrated system where the hybrid system is connected to the load by a bus bar is shown in Figure 1. Methane (fuel) is mixed with a part of anode flue gas and is partially steam reformed in a pre-reformer generating hydrogen. The heat required for endothermic reformation reactions in the pre-reformer is supplied from the SOFC stack through radiation. The gas mixture from the pre-reformer is fed to the anode volume of the SOFC, where the remaining part of the methane is reformed. Compressed atmospheric air is heated in a recuperative heat exchanger and is used as an oxygen source at the cathode side of the SOFC. In the SOFC, electrochemical reactions take place and DC voltage is produced. The rate of the electrochemical reactions depends on the current. A part of the anode flue gas is recycled to supply steam to the pre-reformer. The remaining part of the anode and cathode flue gases is supplied to a combustion chamber where the unused fuel is combusted.

The hybrid system considered here uses a double shaft GT configuration. The combusted gas mixture is expanded in a high pressure turbine (HPT) with variable shaft speed driving the compressor. The HPT flue gas is further expanded to atmospheric pressure in a low pressure turbine (LPT) with constant shaft speed, which is coupled to a synchronous generator producing AC electric power. The expanded gas mixture is used to heat up the compressed air in a heat exchanger. The DC power from the SOFC stack is fed to an inverter which converts DC to AC with a fixed frequency.

R. Kandepu, B. A. Foss and L. Imsland are with Department of Engineering Cybernetics, Norwegian University of Science and Technology, Trondheim, Norway {Rambabu.Kandepu, Bjarne.A.Foss, Lars.Imsland}@itk.ntnu.no

TABLE I

REACTIONS AT ANODE AND CATHODE

At anode	
Reaction	Reaction rate (r_j^{an})
$H_2+O^{2-} \rightarrow H_2O + 2e^-$	r_1^{an}
$CH_4+H_2O \Leftrightarrow CO + 3H_2$	r_2^{an}
$CO + H_2O \Leftrightarrow CO_2+H_2$	r_3^{an}
$CH_4+2H_2O \Leftrightarrow CO_2+4H_2$	r_4^{an}
At cathode	
Reaction	Reaction rate (r_j^{an})
$\frac{1}{2}O_2+2e^- \rightarrow O^{2-}$	r_1^{ca}

The inverter and the generator are connected to a local grid, which is connected to a six branch electric load. Both the SOFC stack and the generator supply the electric load demand on the grid. The power sharing between the SOFC stack and the generator cannot be controlled directly and it depends on the system dynamics. When there is a load change on the grid, the load sharing between the SOFC stack and the generator will change. Typically 60-70% of the total power is supplied by the SOFC stack.

III. MODELING

A. SOFC stack

There are several dynamic, distributed SOFC models reported in the literature. For example, Achenbach [1] developed a three dimensional, dynamic, distributed model for a planar SOFC stack. Chan et al. [2], Thorud et al. [19], Stiller et al. [17] and Magistri et al. [11] all developed distributed, dynamic tubular SOFC models for designs similar to that of Siemens Westinghouse, for use in hybrid systems. In this work a low complexity SOFC model is developed with no explicit regard to the geometry of the cell.

The SOFC converts the chemical energy of the fuel directly into electrical energy. Fuel is supplied to the anode and air is supplied to the cathode. At the cathode-electrolyte interface, oxygen molecules accept electrons coming from the external circuit to form oxide ions. The electrolyte layer allows only oxide ions to pass through and at the anode-electrolyte interface, hydrogen molecules present in the fuel react with oxide ions to form steam and electrons get released. These electrons pass through the external circuit and reach the cathode-electrolyte layer, and thus the circuit is closed. Table I gives the list of reactions that take place at anode and cathode and the corresponding reaction rates notation.

In practice, a number of cells are connected either in series or in parallel or both, according to the voltage requirement. The number of cells in the stack depends on the power demand. In this paper, we assume that all the SOFCs in the SOFC stack operate at identical conditions and there are 1160 cells in the stack. In addition, the following main assumptions have been made in developing the model.

1) All the physical variables are uniform over the SOFC, resulting in a lumped model.
2) There is sufficient turbulence and diffusion within the anode and the cathode for perfect mixing to occur (CSTR).
3) The gas temperatures within the SOFC are the same as the solid; i.e. the thermal inertia of the gases is neglected.
4) For the energy balance, pressure changes within the SOFC are negligible.
5) All gases are ideal.

The dynamic model of a single SOFC is developed using two mass balances (one each for anode and cathode volumes) and one overall energy balance. The two mass balances are;

$$\frac{dN_i^{an}}{dt} = \dot{N}_i^{in,an} - \dot{N}_i^{out,an} + \sum_{j=1}^{M} a_{ij}^{an} r_j^{an},$$

$$\frac{dN_i^{ca}}{dt} = \dot{N}_i^{in,ca} - \dot{N}_i^{out,ca} + a_{i1}^{ca} r_1^{ca},$$

where $i = 1, ..., 7$, refers to the following components: Nitrogen (N_2), Oxygen (O_2), Hydrogen (H_2), Methane (CH_4), Steam (H_2O), Carbonmonoxide (CO), and Carbondioxide (CO_2) and the reactions at anode ($M = 4$) and at cathode are given in Table I. The reaction rates corresponding to the electrochemical reactions (r_1^{ca}, r_1^{an}) are directly related by the current I as

$$r_1^{an} = I/(2F) = r_1^{ca} \tag{1}$$

where F is Faraday's constant. The reaction rates corresponding to the reforming reactions are calculated as proposed by Xu [21]. a_{ij}^{an} and a_{i1}^{ca} denote stoichiometric constants of a component in anode and cathode respectively. It is assumed that the exhaust flows at the anode and cathode outlets can be described by the choked exhaust flow equation. This means that the mass flow rate of the exhaust flow at the anode (cathode) depends on the pressure difference between the pressure inside the anode (cathode) and the pressure at the outlet [13]. The partial pressures, volume, and temperature both in anode and cathode are assumed to be related by the ideal gas equation. The energy balance accounts for the whole SOFC volume, and is given by [18], [10]:

$$\begin{aligned} C^s \frac{dT}{dt} = &\sum_{i=1}^{N} \dot{N}_i^{in,an} (\Delta\overline{h}_i^{in,an} - \Delta\overline{h}_i) \\ &+ \sum_{i=1}^{N} \dot{N}_i^{in,ca} (\Delta\overline{h}_i^{in,ca} - \Delta\overline{h}_i) \\ &- \sum_{j=1}^{M} \Delta\overline{h}_j^{rx} r_j^{an} - P_{DC} - P_{rad} \end{aligned} \tag{2}$$

where P_{DC} is the amount of DC power produced by the SOFC, P_{rad} is the amount of radiation heat given from the SOFC, $\Delta\overline{h}_i$ is the molar specific enthalpy of a component, $\Delta\overline{h}_j^{rx}$ is the molar specific enthalpy change of a reaction j, C^s is the SOFC solid heat capacity, T is SOFC solid temperature, $N = 7$ is the number of components, $\Delta\overline{h}_i^{in,an}$ and $\Delta\overline{h}_i^{in,ca}$ denote molar specific enthalpy of a component at anode cathode inlets, respectively.

In (2), the temperature dynamics of gases are neglected as they are fast compared to the temperature changes of the

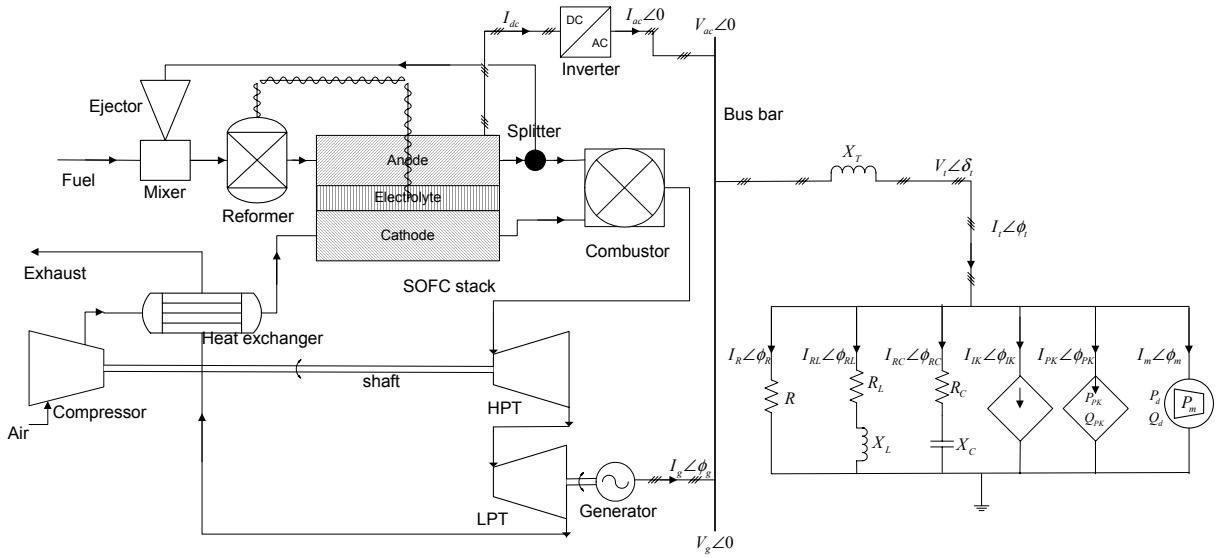

Fig. 1. SOFC-GT hybrid system integrated with autonomous power system

solid. As the SOFC operating temperature is higher than that of the surroundings, there is always some loss due to radiation. The operating cell voltage is given by

$$V = E^{OCV} - V_{loss} \tag{3}$$

where the open circuit voltage (E^{OCV}) of the cell is given by the *Nernst equation* [8], and V_{loss} is the voltage loss which includes ohmic, concentration and activation losses. Moreover, Air Utilization (AU) and Fuel Utilization (FU) are defined as

$$\text{AU} = 1 - \frac{\dot{N}_{O_2}^{out}}{\dot{N}_{O_2}^{in}}, \quad \text{FU} = 1 - \frac{\dot{N}_{H_2}^{out}}{\dot{N}_{H_2}^{in}}. \tag{4}$$

The AU and FU are included in the model as they are identified as important variables in representing the SOFC state [19]. Recycle ratio is defined as the ratio of the fuel flow recycled to the fuel flow at the anode outlet.

In [7], the low complexity SOFC model is evaluated against a detailed model developed in [19], [17]. The comparisons indicate that the low complexity model is good enough to approximate the important dynamics of the SOFC and can hence be used for operability and control studies.

B. Reformer

A reformer is used to convert methane into hydrogen by steam reforming. It is a fixed volume reactor having two inlets, one for methane and the other for steam and one outlet. The assumptions made in the model development of the reformer are same as that of the SOFC. The dynamic model is developed using one mass balance and one energy balance. The three reformation reactions considered are given in Table I. The reformation is a highly endothermic process, so heat must to be supplied to the reactor. As the SOFC operates at a high temperature, there is radiation from the SOFC stack and this can be supplied to the reformer by using a suitable mechanical design. The operating temperature of the reactor is in the range $500°C - 700°C$.

C. Heat exchanger

A very simple model of a counter-flow heat exchanger is used, in which the amount of the heat exchanged depends on the heat transfer coefficient of the exchanger wall and also on the average temperature difference between the hot and cold streams. A first order transfer function describes the dynamics of the temperatures of both the streams. The following assumptions were made,

1) The model is lumped. All the physical parameters are assumed to be uniform over the heat exchanger.
2) There is no pressure loss within the heat exchanger.

D. Combustion chamber

The combustion chamber as shown in Figure 1 has $n_{in} = 2$ inlet streams and one outlet stream. It burns the fuel coming from all the inlet flows in the presence of air. The operating conditions will always be such that there is surplus oxygen available for complete combustion due to the fact that air mass flow rate is much larger than the fuel mass flow rate. In this model, the fuel can be methane, hydrogen or carbonmonoxide or a mixture of these fuels. The following reactions are being considered during the combustion.

$$\begin{aligned} 2H_2 + O_2 &\rightarrow 2H_2O \\ CH_4 + 2O_2 &\rightarrow 2H_2O + CO_2 \\ 2CO + O_2 &\rightarrow 2CO_2 \end{aligned} \tag{5}$$

The following assumptions are made:

1) The pressures of all the inlet flows are the same.
2) As the combustion process is very rapid, it is modeled as an instantaneous process and complete combustion is assumed.

3) The model is a bulk model, i.e. all physical variables are assumed to be uniform over the combustion chamber.
4) There is a 2% pressure loss in the combustor volume.

The following mass and energy balances are used for the control volume:

$$\sum_{k=1}^{n_{in}} \dot{N}_i^{in,k} + \sum_{j=1}^{n_{rx}} a_{ij} r_j = \dot{N}_i^{out}, \quad i = 1...7, \; n_{rx} = 3$$

$$\sum_{k=1}^{n_{in}} \sum_{i=1}^{N} (\dot{N}_i^{in,k} \Delta\overline{h}_i^{in,k} - \sum_{i=1}^{N} \dot{N}_i^{in,k} \Delta\overline{h}_i) - \sum_{j=1}^{M_c} \Delta\overline{h}_j^{rx} r_j = 0$$

where $N = 7$ is the number of components, $M_c = 3$ is the number of reactions as given in (5) and the variables notation is similar as in (2) but refer to the combustion chamber.

E. Gas turbine

Compressor and turbine models are based on steady state performance map characteristics [16]. The map is modeled using polynomials of 4th and 5th order for reduced mass flow, pressure and efficiency as functions of reduced shaft speed and operation line. The following are the assumptions made in both the compressor and turbine models:

1) The process has constant isentropic efficiency.
2) The working fluid satisfies the ideal gas equation.

A shaft model accounts for the dynamics of the rotating mass in the gas turbine system which is modeled as

$$\dot{\omega} = P_b/(I\omega) \tag{6}$$

where P_b is the power balance across the shaft, I is the moment of inertia of the rotating mass and ω is the angular velocity of the shaft.

F. Inverter

A simple model of inverter is developed with the following assumptions:

1) Power loss is negligible.
2) Pulse Width Modulation (PWM) technique is used to control the AC output voltage and frequency. The controller dynamics are neglected as they are very fast compared to the hybrid system dynamics.
3) The inverter supplies AC power at unity power factor.

The power balance on both sides is given by

$$P_{dc} = V_{ac} I_{ac}. \tag{7}$$

G. Synchronous generator

The per-phase equivalent circuit of the synchronous generator is shown in Figure 2 taken from [20]. The magnitude of the electro-motive force (EMF) induced in each phase is assumed to be directly proportional to the shaft speed (ω_g) and field current (I_{fg}),

$$E_g = k_g I_{fg} \omega_g \tag{8}$$

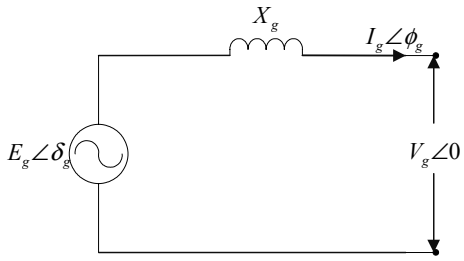

Fig. 2. Per-phase equivalent circuit of synchronous generator

where k_g is the proportionality constant. The open circuit voltage $V_g\angle 0$, which is taken as the reference in phasor notation, and $E_g\angle\delta_g$ are related as

$$E_g\angle\delta_g = V_g\angle 0 + X_g\angle 90^\circ I_g\angle\phi_g \tag{9}$$

where $I_g\angle\phi_g$ is the generator current, X_g is the stator per-phase reactance in ohms. It is assumed that there is 2% power loss in conversion from mechanical to electrical form which includes rotational loss, copper loss and magnetizing loss. The generator is connected to a power turbine which runs at a constant speed. Hence the frequency of the AC supply from the generator is assumed constant. The real and reactive powers supplied by the generator are given by

$$\begin{aligned} P_g &= V_g I_g \cos\phi_g \\ Q_g &= V_g I_g \sin\phi_g. \end{aligned} \tag{10}$$

H. Autonomous power grid

The integrated SOFC-GT hybrid system with the autonomous power grid is shown in Figure 1. The model of the grid and load is chosen such that the level of complexity is comparable to the SOFC-GT hybrid system models. The bus bar voltage is fixed at $230V$ and is taken as the reference in phasor notation. We assume that the generator field current is controlled such that the generator terminal voltage $V_g\angle 0$ equal to the bus bar voltage $V_{ac}\angle 0$. The bus bar is connected to the load by transmission lines of reactance X_T. The load is represented by six parallel branches with different components in each branch as shown in Figure 1. It is categorized into 4 types of loads; constant impedance, constant current, constant power and induction motor load. The constant impedance, constant current and constant power load represent the residential loads such as lights, water heaters, ovens etc. The induction motor load is considered to represent an industrial load [12]. The constant impedance load is represented by the first three branches with resistive, inductive and capacitive loads. The fourth and fifth branches represent the constant current and constant power loads respectively. The sixth branch represents the induction motor load. The total load current $I_t\angle\phi_t$ is the sum of the currents from the inverter and the synchronous generator,

$$I_t\angle\phi_t = I_{ac}\angle 0 + I_g\angle\phi_g. \tag{11}$$

As it is assumed that the inverter supplies power at unity power factor, generator supplies the load reactive power and

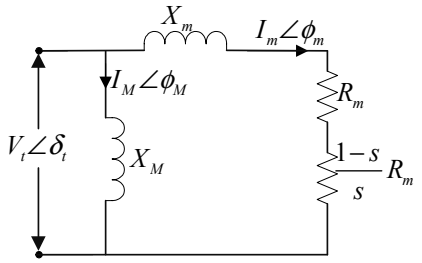

Fig. 3. Equivalent circuit of induction motor

transmission line reactive power. The load voltage $V_t\angle\delta_t$ is given by

$$V_t\angle\delta_t = V_{ac}\angle 0 - JX_T I_t\angle\phi_t. \quad (12)$$

The first three branches of the load (R, RL, RC branches) are used to model different constant impedance loads. The currents in these branches are given by

$$\begin{aligned} V_t\angle\delta_t &= RI_R\angle\phi_R \\ V_t\angle\delta_t &= (R_L + X_L\angle 90^\circ)I_{RL}\angle\phi_{RL} \\ V_t\angle\delta_t &= (R_C - X_C\angle 90^\circ)I_{RC}\angle\phi_{RC}. \end{aligned} \quad (13)$$

The fourth branch is used to model constant current loads where the current $I_{IK}\angle\phi_{IK}$ is assigned a constant value. The fifth branch is used to model constant power loads where real and reactive powers (P_{PK},Q_{PK}) are assigned constant values and the current $I_{PK}\angle\phi_{PK}$ is calculated by

$$\begin{aligned} P_{PK} &= V_t I_{PK}\cos(\phi_{PK} - \delta_t) \\ Q_{PK} &= V_t I_{PK}\sin(\phi_{PK} - \delta_t). \end{aligned} \quad (14)$$

The last branch is used to model induction motor, whose equivalent circuit is shown in Figure 3 [5]. Assuming the magnetizing inductance is large, i.e. $X_M \to \infty$, the magnetizing current $I_M\angle\phi_M$ is neglected [5]. The induction motor model equations are then given by,

$$\begin{aligned} \frac{ds}{dt} &= \frac{1}{I\omega_o^2}\left(\frac{P_m}{1-s} - P_d\right) \\ V_t\angle\delta_t &= (\frac{R_m}{s} + X_m\angle 90^\circ)I_m\angle\phi_m \\ P_d &= V_t I_m\cos(\phi_m - \delta_t) \\ Q_d &= V_t I_m\sin(\phi_m - \delta_t) \end{aligned} \quad (15)$$

where I is moment of inertia of induction motor, ω_o is stator frequency, P_m is mechanical load power on the induction motor, P_d and Q_d are real and reactive power from induction motor, and s is slip given by $s = \frac{\omega_o - \omega_m}{\omega_m}$ where ω_m is induction motor speed.

All the components of the hybrid system and the autonomous power system are modeled in the modular modeling environment gPROMS [3].

IV. CONTROL AND SIMULATION

An integrated open-loop system is simulated with a set of nominal, realistic parameters resulting in a nominal state partially shown in Table II. As may be expected, there is a need to design a control system to compensate for disturbances in the load. The system goes unstable for certain load disturbances which further accentuate the need for a controller design. The open loop simulations further show the importance of including the grid with connected load model since the dynamics and the sensitivity of some important variables of the hybrid system to the load disturbances are different from the situation, when the grid with connected load is represented by a power sink.

TABLE II
NOMINAL STATE OF THE SYSTEM

Variable	Value
SOFC current	250A
fuel flow rate	0.007kg/s
SOFC temperature	1350K
SOFC cell voltage	0.657V
SOFC stack power	191kW
generator power	87kW
air mass flow rate	0.445kg/s
AU	0.23
FU	0.85
recycle ratio	0.54
reforming degree	0.38
steam/methane ratio	2
I_t	1248A
V_t	222V
Induction motor slip	0.1

As the main source of the power in the hybrid system is the fuel flow, fuel flow must be controlled to match the power demand in case of any load changes. Since it is not always possible to know the load in advance, any load change is treated as a disturbance to the controller. As the bus bar voltage is fixed when there is a load change, the current and the FU in SOFC vary. The FU cannot be varied too much since it may cause uneven temperature and voltage distributions inside the cell [16]. Hence FU is taken as a controlled variable, where it is assumed that a perfect observer is available to estimate FU.

A load change can affect the SOFC temperature to change beyond the material constraints [8] [16]. Hence the SOFC temperature should be controlled during the load changes. As there is no other free manipulated variable available for this purpose, a slight change must be made in the process design. After analyzing three different possible choices for the extra manipulated variable, air blow off at compressor outlet is found to be superior in terms of control authority, compared to air bypass across the heat exchanger and additional fuel to the combustion chamber. The control structure is selected from the physical understanding of the process and RGA analysis [15] based on the linearized system confirms it. The non-linear system is linearized at its nominal state given in Table II, and decentralized PI controllers are tuned according to the rules given by Skogestad [14]. The PI controllers are then implemented on the non-linear system.

To evaluate the proposed control structure, the following simulation scenario is used. The system is simulated at the nominal state for one sec. After one sec, the following disturbances are applied: the mechanical load on the induction

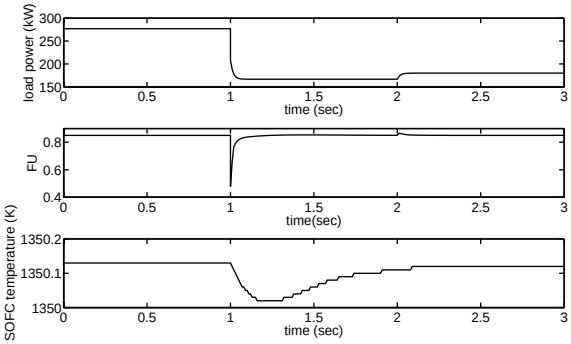

Fig. 4. Mechanical load change, FU, and SOFC temperature during simulation

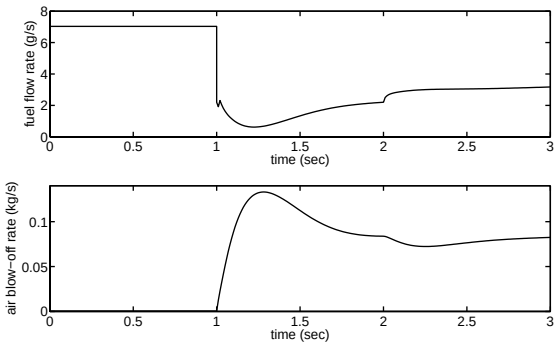

Fig. 5. Plant inputs during simulation

motor (P_m) is decreased to 10%, R is increased by 5 times, I_{IK} is decreased to 10% and P_{PK} is decreased to 10% which constitutes 40% load decrease on the system. After 2 secs, the P_m is increased to 50%. The total load change, FU and SOFC temperature profiles during the simulation are shown in Figure 4. The plant inputs, i.e. fuel flow and air blow-off during the simulation are shown in Figure 5. When there is a load decrease, correspondingly the current and amount of fuel utilized in the SOFC is decreased, which decreases the FU. To maintain FU constant at 0.85, the fuel flow rate is decreased as shown in Figure 5. When the current is decreased in SOFC, the electrochemical reactions rate is decreased which decreases the SOFC temperature. To maintain the SOFC temperature at a constant value the air mass flow rate through the SOFC should decrease meaning that the air blow-off rate must increase as shown in Figure 5. At the nominal state a small non-zero air blow-off rate is chosen to be able to control the SOFC temperature for any small increase in the load at the nominal value. For the 40% load change, the air blow-off rate constitutes about 18% of the total air mass flow rate which may cause a decrease in system efficiency. This is because of the strict control of the SOFC temperature at the nominal value. If the SOFC temperature is chosen to vary in some bounds around the nominal value, the air blow-off utilization can be optimized to a higher system efficiency. However, from the control point of view the proposed control structure gives satisfactory results as seen from Figures 4 and 5.

V. CONCLUSIONS AND FURTHER WORK

A model of complete power system where a SOFC-GT hybrid system is connected to grid with connected load is developed to include the important interactions between the grid and the hybrid system. A control structure with PI controllers shows that satisfactory results can be obtained, but the main disadvantage is that the system efficiency will be reduced with the use of blow-off to control the SOFC temperature during part-load operation.

Future work will focus on optimizing the control design to reduce the air-blow off utilization to control the SOFC temperature to increase the system efficiency at part load operation. While the present paper assumed a two-shaft GT design, we are also looking at integration with a *single-shaft* GT design, which poses further challenge for a control design. A single-shaft GT offers the possibility of avoiding air blow-off by controlling shaft speed directly. It will also be focussed on designing a control structure for start up and shut down operations.

VI. ACKNOWLEDGMENTS

Financial support from The Gas Technology Center, NTNU-SINTEF and NFR is acknowledged. We also thank Dr. Kjetil Uhlen and Dr. Vinay Kariwala for fruitful discussions.

REFERENCES

[1] E. Achenbach. Three-dimensional and time-dependent simulation of a planar solid oxide fuel cell stack. *Journal of Power Sources*, 1994.

[2] S.H. Chan, H.K. Ho, and Y. Tian. Multi-level modeling of sofc-gas turbine hybrid system. *International Journal of Hydrogen Energy*, 2003.

[3] gPROMS (2004). gPROMS introductory user guide. *Process Systems Enterprise Ltd.*, 2004.

[4] C. J. Hatziadoniu, A. A. Lobo, F. Pourboghart, and M. Daneshdoost. A simplified dynamic model of grid-connected fuel-cell generators. *IEEE transactions on power delivery*, 17(2), April 2002.

[5] D. J. Hill. Nonlinear dynamic load models with recovery for voltage stability studies. *IEEE transactions on power systems*, 8(1), February 1993.

[6] D. Jensen and J. W. Dijkstra. Co2 capture in sofc-gt systems. *Proceedings of second annual conference on Carbon Sequestration*, May 2003.

[7] R. Kandepu, L. Imsland, B. A. Foss, C. Stiller, B. Thorud, and O. Bolland. Control-relevant sofc modeling and model eveluation. *Proceedings of ECOS*, 2005.

[8] J. Larminie and A. Dicks. *Fuel Cell Systems Explained*. Wiley, England, 2003.

[9] J. Pålsson, A. Selimovic, and L. Sjunnesson. Combined solid oxide fuel cell and gas turbine systems for efficient power and heat generation. *Journal of Power Sources*, 2000.

[10] M. D. Lukas, K. Y. Lee, and H. Ghezel-Ayagh. An explicit dynamic model for direct reforming carbonate fuel cell stack. *IEEE Transactions on Energy Conversion*, 16(3), September 2001.

[11] L. Magistri, F. Trasino, and P. Costamagna. Transient analysis of a solid oxide fuel cell hybrids part a: fuel cell models. *Journal of Power Sources*, 2004.

[12] I. R. Navarro. *Dynamic power system load - Estimation of parameters from operational data*. Media-Tryck, Lund, 2005.

[13] J. Padulles, G.W. Ault, and J. R. McDonald. An integrated sofc dynamic model power systems simulation. *Journal of Power sources*, pages 495–500, 2000.

[14] S. Skogestad. Simple analytic rules for model reduction and pid controller tuning. *Journal of process control*, 2005.
[15] S. Skogestad and I. Postlethwaite. *Multivariable feedback control: Analysis and Design*. Wiley, USA, 1996.
[16] C. Stiller, B. Thorud, O. Bolland, K. Rambabu, and L. Imsland. Control strategy for a solid oxide fuel cell and gas turbine hybrid system. *submitted to Journal of Power Sources*, 2005.
[17] C. Stiller, B. Thorud, S. Seljebø, Ø. Mathisen, H. Karoliussen, and O. Bolland. Finite-volume modeling and hybrid-cycle performance of planar and tubular solid oxide fuel cells. *Journal of Power Sources, 141, 227-240*, 2005.
[18] P. Thomas. *Simulation of Industrial Processes For Control Engineers*. Butterworth-Heinemann, Wobourn, MA, USA, 1999.
[19] B. Thorud, C. Stiller, T. Weydahl, O. Bolland, and H. Karoliussen. Part-load and load change simulation of tubular sofc systems. *Proceedings of Fuel Cell Forum, Lucerne, 28 June-2 July*, 2004.
[20] L. A. A. Warnes. *Electronic and Electrical Engineering*. Macmillan, London, 1994.
[21] J. Xu and G. F. Froment. Methane steam reforming, methanation and water-gas shift: I. intrinsic kinetics. *AIChE Journal*, 1989.